An electronic Raman scattering study on $YBa_2Cu_3O_7$ in the superconducting state

1994 J. Phys.: Condens. Matter 6 1057

(http://iopscience.iop.org/0953-8984/6/5/016)

J. Phys.: Condens. Matter 6 (1994) 1057–1064. Printed in the UK

An electronic Raman scattering study on $YBa_2Cu_3O_7$ in the superconducting state

A Sacuto†, M A Kanehisa† and O Gorochov‡

† Laboratoire de Physique des Solides, associé au CNRS, Université Pierre et Marie Curie, Tour 13-E2, 4 Place Jussieu, 75252 Paris Cédex 05, France

‡ Laboratoire de Physique des Solides de Bellevue, CNRS, 1 Place Aristide Briand, 92195 Meudon Principal Cédex, France

Received 19 July 1993, in final form 15 October 1993

Abstract. An electronic Raman scattering study at low frequency has been performed on $YBa_2Cu_3O_7$ single crystals below and above the transition temperature T_c. The intensity of the electronic continuum at low frequency shows a drastic change with temperature variation. The differential cross section calculation based on the Green's function formalism in the random-phase approximation has permitted us to isolate the low-energy electronic contribution from the phonons and point out its behaviour as a function of temperature. A decrease of the electronic contribution in the superconducting state compared with that in the normal state then appears, which it is possible to assign to the pairing of the free carriers near the Fermi energy. However, this low-energy electronic contribution persists well below T_c, suggesting the existence of electronic states near the Fermi energy even in the superconducting state.

1. Introduction

Since the discovery of $YBa_2Cu_3O_7$ high-T_c superconductors, many Raman scattering studies have been devoted to the analysis of the phonons and electronic properties of these compounds in the normal and superconducting states. Early investigations [1–4] pointed out evidence for a strong electron–phonon interaction characterized by Fano [5] asymmetric lineshapes of the A_g normal mode at 117 cm^{-1} and the B_{1g} normal mode at 336 cm^{-1}. They have also shown the presence, below T_c, of two strong electronic contributions of A_g and B_{1g} symmetry assigned to gap anisotropy with two quasi-particle pair breaking peaks at $\omega = 530$ cm^{-1} and $\omega = 336$ cm^{-1}, respectively. Recent Raman measurements [6, 7] have not found a transition temperature dependence for the electronic continuum peak centred at 530 cm^{-1} which persists well above T_c. This means that this electronic feature is not related to the superconducting gap. However, a drastic change in the electronic Raman scattering at low frequency, below the B_{1g} mode, has been observed on passing through the transition temperature.

In this paper, we do not attempt to determine the superconducting energy gap, which remains an open question and raises many discussions. Even on the determination of the superconducting gap by Raman spectroscopy, based upon the behaviour of the optical phonon linewidth below and above the 2Δ gap energy, the opinions are divided. One [8] reports the superconducting energy gap at $2\Delta \simeq 5\ k_B T_c$ whereas another [9] finds $2\Delta \simeq (6\text{–}7)\ k_B T_c$. Moreover, the Raman gap energy estimates are in disagreement with the infrared energy gap measurements [10], which give $2\Delta \simeq 8\ k_B T_c$. Our purpose is thus to study the electronic Raman scattering behaviour at low frequency, below the B_{1g}

0953-8984/94/051057+08$07.50

normal mode, in the normal and superconducting states. In order to analyse the low-frequency electronic contribution behaviour with temperature variation, we have calculated the differential scattering cross sections $d\sigma(\omega)/d\omega\, d\Omega$ of the spectrum below the B_{1g} mode. The Green's function formalism [11–13] of first-order Raman scattering in the random-phase approximation (RPA) was used and we have taken into account the interactions of the two phonons at 117 cm^{-1} and 152 cm^{-1} with the electronic continuum and their mutual interaction via electronic excitations.

2. Experimental arrangement

Raman spectroscopy investigations were performed on $YBa_2Cu_3O_{7-\delta}$ single crystals with $\delta \simeq 0$. Crystals were grown in a gold crucible, from a melted phase containing an excess of CuO and BaO, by the flux technique [14]. Their typical sizes are $1.0 \times 0.5 \times 0.1$ mm^3. These samples characterized with x-ray diffraction techniques are orthorhombic ($a \neq b \neq c$) and present twin free domains in the a–b plane. The crystals are superconductors with a critical temperature $T_c = 92$ K and a transition width of 1 or 2 K. Raman measurements were carried out with a U-1000 Jobin Yvon double monochromator, using a 514.52 nm line of an ionized Argon laser. A photomultiplier tube EMI 9863B was connected to a microcomputer for data collection. Brewster's conditions were realized, to minimize Rayleigh scattering, and the scattered light was collected along the surface normal to the a–b plane. The incident and scattered electric field directions are parallel, contained in the a–b plane and denoted by x'. (x' has not got a peculiar axis orientation since the crystal is twinned in the a–b plane.) The samples were cooled in a liquid helium cryostat and the temperature was controlled by a SMC-TBT regulator. The intensity of the incident beam was maintained below roughly 10 W cm^{-2}, in order to minimize possible thermal damage.

3. Results and discussion

Electronic Raman scattering at low frequency, below the B_{1g} normal mode, as a function of temperature in ($x'x'$) polarization is illustrated in figure 1. The two A_g normal modes at 117 cm^{-1} and 152 cm^{-1} are assigned [2] to the vibration along the c axis of the barium atoms and the Cu2 copper atoms, respectively. They both present an asymmetric lineshape, characteristic of a strong electron–phonon interaction. The B_{1g} mode, assigned [2] to the out-of-phase motion of the O2–O3 oxygen atoms along the c axis, is also strongly coupled to the electronic excitations, and stiffens as the temperature increases [1, 2, 8]. A drastic change in the electronic continuum at low frequency is observed with temperature variation. The electronic continuum intensity increases as the temperature increases in the superconducting state and becomes stable near T_c. As the Raman analysis is performed in the low-energy range, only the initial and final states, just below and just above the Fermi energy level, have been considered in the electronic Raman scattering process. Band structure calculations [15–16] have pointed out that most of the bands crossing the Fermi energy level originate from the CuO chains and CuO_2 planes. The low-energy excitations detected on the Raman spectra are thus predominantly coming from the CuO chains and CuO_2 planes bands. In order to extract the low-energy electronic contribution and to analyse its variation as a function of temperature, we have calculated the differential Raman scattering cross section $d\sigma(\omega)/d\omega\, d\Omega$ of the spectrum below the B_{1g} mode, taking into account the interaction of

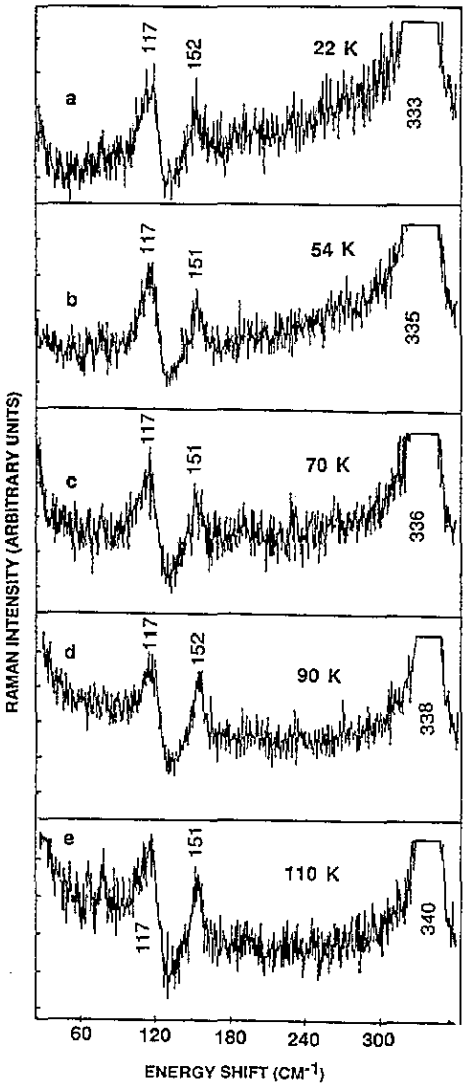

Figure 1. Electronic Raman scattering at low frequency, below the B_{1g} normal mode, versus temperature in $(x'x')$ polarization: a, $T = 22$ K; b, $T = 54$ K; c, $T = 70$ K; d, $T = 90$ K; e, $T = 110$ K.

each phonon (the two optical phonons at 117 cm^{-1} and 152 cm^{-1}) with the electronic continuum and their mutual interaction via the electronic continuum.

As it has already been used in the Raman theory of interference [11–13], the differential cross section of first-order Raman scattering is related to the Fourier transform of the correlation function which describes, in our case, the quantum interferences between the two optical phonons and the electronic continuum. In the long-wavelength limit ($q \to 0$), the differential cross section

$$d^2\sigma/d\Omega\, d\omega \propto \langle [A\rho_1(\omega) + B\rho_2(\omega) + \lambda\rho_e(\omega)][A\rho_1(0) + B\rho_2(0) + \lambda\rho_e(0)]\rangle_T$$

where ρ_1 and ρ_2 are the charge densities associated to the first and second phonon, ρ_e is the

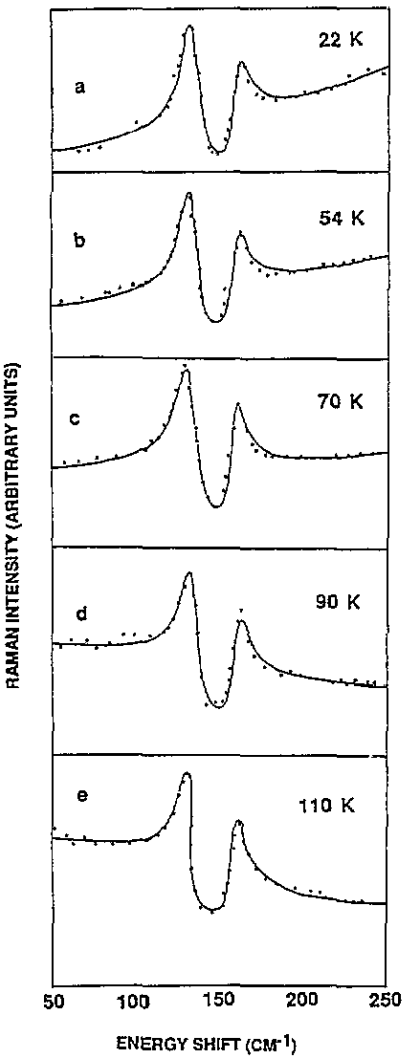

Figure 2. Fits of the calculated differential cross section to the Raman spectra in $(x'x')$ polarization between 50 and 250 cm^{-1}: a, T = 22 K; b, T = 54 K; c, T = 70 K; d, T = 90 K; e, T = 110 K.

electronic density fluctuation, A, B and λ represent the intensity ratios of each contribution and $< \ldots >_T$ denotes the thermal average. Using the same method of calculation as in [13], we have expressed the correlation function $\rho(\omega)$ in terms of a composite Green's function $D(\omega)$ such that

$$\rho(\omega) = -\operatorname{Im}[D(\omega)(n(\omega, T) + 1)]$$

with

$$D(\omega) = (A^2 D_{11}(\omega) + B^2 D_{22}(\omega) + AB(D_{12}(\omega) + D_{21}(\omega)) + 2\lambda(AD_{e1}(\omega) + BD_{e2}(\omega)) + \lambda^2 D_{ee}(\omega))$$

and where $n(\omega, T)$ is the Bose factor.

The $D_{\alpha\beta}$, $D_{\alpha e}$, $D_{\beta e}$ and D_{ee} ($\{\alpha, \beta\} = \{1, 2\}$) propagators are derived, in the RPA, from the infinite set of Feynman's diagrams. Let us denote the electronic polarization Green's function F by, the frequencies of the first and second pure phonons by ω_1 and ω_2, respectively, and the dimensionless e–ph coupling constants associated, to the first and second phonons by g_1 and g_2, respectively. For the case under consideration, it is a good approximation to neglect the momentum dependence of the coupling constant g_α, since $q \to 0$. The $D_{\alpha,\beta}$, $D_{\alpha e}$, $D_{\beta e}$ and D_{ee} are then described by

$$D_{\alpha\beta} = \delta_{\alpha\beta} D_\alpha + g_\alpha g_\beta D_\alpha D_\beta F[1 - F(g_1^2 D_1 + g_2^2 D_2)]^{-1}$$

$$D_{\alpha e} = g_\alpha D_\alpha F[1 - F(g_1^2 D_1 + g_2^2 D_2)]^{-1}$$

$$D_{ee} = F[1 - F(g_1^2 D_1 + g_2^2 D_2)]^{-1}$$

where D_α is the propagator of a single phonon defined by

$$D_\alpha \lim_{\delta \to 0} \omega_\alpha[(\omega - \omega_\alpha + i\delta)^{-1} + (\omega + \omega_\alpha - i\delta)^{-1}].$$

As the separation in energy of the two optical phonons is small compared with their sum and the energy range of interest is near the phonon energies, we can consider the first term of the phonon propagator. Moreover, as the optical phonon energies fall inside the electron–hole continuum, the electronic polarization Green's function F can be considered purely as imaginary and can be expressed as $F = if(\omega, T)$, where $f(\omega, T)$ is a smooth function of energy and temperature. The intensity of the Raman scattering corresponding to the above correlation function, and normalized to the first phonon intensity I_1, is then described by

$$I(\omega, T) = [I_1 g_1^2 f^2(\omega, T)/\Delta_1^2\Delta_2^2 + (g_1^2\Delta_2 + g_2^2\Delta_1)^2 f^2(\omega, T)] \times (\Delta^2 - 2\lambda\Delta_1\Delta_2\Delta + \lambda^2\Delta_1^2\Delta_2^2)(n(\omega, T) + 1)$$

where

$$\Delta = Ag_1\Delta_2 + Bg_2\Delta_1 \qquad A = 1 \qquad \Delta_1 = 1 - \omega/\omega_1 \qquad \text{and} \qquad \Delta_2 = 1 - \omega/\omega_2.$$

By fitting the calculated Raman scattering intensity to the experimental spectrum in the 25–250 cm^{-1} range at $T = 22$ K, we have fixed the parameters λ, B, I_1, ω_1 and ω_2. These parameters, listed in table 1, are assumed to be, to a first approximation, independent of temperature. The e–ph coupling constants (g_1, g_2) and the imaginary part of the Green's function $f(\omega, T)$ have been chosen for the fitting of the Raman scattering intensity with the temperature variation. These fits are displayed in figure 2 and we can notice that the agreement between theory and experiment is good. The g_1 and g_2 coupling constants related to the first and second phonons are listed in table 2. The signs of the e–ph matrix elements (g_1, g_2) could appear to be without meaning since they depend on the signs of the scattering amplitudes (AB) which are assumed, arbitrarily, to be positive. However, the opposite sign for their product (Ag_1, Bg_2) is significant and some more investigations in this domain are needed, g_1 and g_2 are almost constant as the temperature increases, meaning that the effects of finite temperature on these coefficients is weak, whereas the electronic contribution $f(\omega, T)$, illustrated in figure 3, displays a drastic change as the temperature passes through T_c. We can therefore clearly differentiate the electronic contribution behaviour in the superconducting state ($T = 22$ K, $T = 54$ K, $T = 70$ K) from the behaviour in the

Table 1. Fixed parameters

B	I_1	ω_1 (cm^{-1})	ω_2 (cm^{-1})	λ
0.7	2.5	119	151	2

Table 2. Electron–phonon coupling constants as a function of temperature.

T (K)	g_1	g_2
22	-0.255 ± 0.001	0.184 ± 0.001
54	-0.244 ± 0.001	0.189 ± 0.001
70	-0.222 ± 0.001	0.178 ± 0.001
90	-0.212 ± 0.001	0.175 ± 0.001
110	-0.208 ± 0.001	0.177 ± 0.001

normal state ($T = 110$ K), or near the transition temperature ($T = 90$ K). A more intensive electronic contribution $f(\omega, T)$ is then detected in the normal state (or near T_c) than in the superconducting state.

According to electronic Raman scattering theory [17] in conventional superconductors, based on the Bardeen, Cooper, Schrieffer model, there is no scattering by free carriers in the superconducting state, unless the energy transferred, $\omega_i - \omega_d$, exceeds $2\Delta_k$. Moreover, when the coherence length ξ is small compared with the optical penetration depth δ, as in the case of $YBa_2Cu_3O_7$ ($\xi \simeq 10$ Å, $\delta \simeq 1000$ Å for $\lambda = 514.52$ nm), the light scattering cross section is equal, for an isotope 2Δ gap energy, to 0 for $0 < \omega < 2\Delta$ and varies as $\Delta^2/[\omega^2(\omega^2 - 4\Delta^2)^{1/2}]$ for $\omega \geqslant 2\Delta$. This predicts no electronic Raman scattering below 2Δ and an electronic continuum peak for $\omega = 2\Delta$, due to the direct Raman scattering from quasi-particle pairs. In this new high-T_c superconductor we observe a decrease of the low-energy electronic excitations in the superconducting state compared with the normal state, but no break delimiting a spectral region without Raman scattering, and no electronic continuum peak due to the direct 'Cooper pair breaking' as has been detected in the A15 compounds, such as V_3Si or Nb_3Sn [17, 18]. It is consequently very difficult to determine the energy gap in $YBa_2Cu_3O_7$ compounds by observation of the electronic continuum variation with temperature. However, recent investigations [19] on $Bi_2Sr_2CaCu_2O_8$ have shown that it is possible to obtain a completely developed clean gap for B_{1g} polarization while, for others, only a reduced density of states is compatible with the data at low energies. Unfortunately, this is not the case for $YBa_2Cu_3O_7$ (see, for example, [3, 4]). The decrease of the electronic Raman scattering of $YBa_2Cu_3O_7$ at low frequency in the superconducting state, in comparison with the normal state, suggests pairing of the electronic states near the Fermi energy. However, the electronic Raman scattering below T_c is not zero, as shown in figure 3, and the barium normal mode presents an asymmetric lineshape characteristic of the interaction between a single phonon and an electronic continuum. It then appears that electronic states persist near the Fermi energy in the superconducting state and this observation is confirmed by tunnelling measurements [20], which present for $T \ll T_c$ a reproducible finite zero-bias conductance. In fact, there exist two kinds of free carriers in $YBa_2Cu_3O_7$, those related to the CuO_2 planes and those related to the CuO chains. If we assume, as already mentioned in [21], that it is essentially the carriers in the CuO_2 planes which are involved in the pairing process, the carriers in the chains could partially explain the presence of the electronic excitations in the Raman spectra well below T_c. However, carrier contributions coming from the CuO_2 planes are not excluded, because, as mentioned in [19], the Raman spectra of the $Bi_2Sr_2CaCu_2O_8$ structure which have no CuO chains, but

possess CuO_2 planes, also exhibit low-energy scattering excitations well below T_c in *a–b* plane polarization.

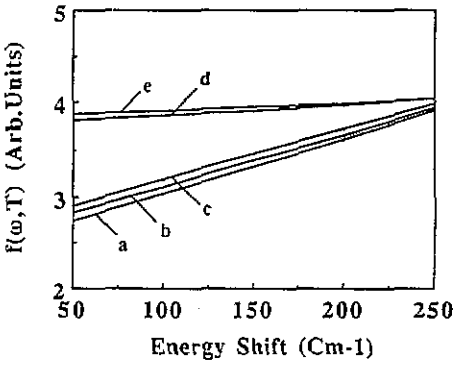

Figure 3. Electronic Raman scattering behaviour as a function of temperature in the 50–250 cm^{-1} range, obtained from the Raman spectra in $(x'x')$ polarization: a, $T = 22$ K; b, $T = 54$ K; c, $T = 70$ K; d, $T = 90$ K; e, $T = 110$ K.

4. Conclusion

An electronic Raman scattering study as a function of temperature, in *a–b* plane polarization, shows that the electronic continuum below the B_{1g} normal mode presents a drastic change as the temperature increases to T_c. The differential cross section calculation, based on the Green's function formalism, has permitted us to separate the phononic structure from the electronic continuum, and to present the electronic contribution $f(\omega, T)$ at low energy and its behaviour as a function of temperature. A decrease of the low-energy electronic contribution then appears in the superconducting state compared with the normal state, which can be attributed to the pairing of the free carriers near the Fermi energy. However, this electronic contribution persists well below T_c, suggesting the existence of electronic states near the Fermi energy, even in the superconducting state.

Acknowledgments

It is a pleasure to thank Professors J Ruvalds, M Balkanski and J Labbe for their help and discussions.

References

[1] Macfarlane R M, Rosen H and Seki H 1987 *Solid State Commun.* **63** 831
[2] Cooper S L, Klein M V, Pazol B G, Rice J P and Ginzberg D M 1988 *Phys. Rev.* B **37** 5920
[3] Cooper S L, Slakey F, Klein M V, Rice J P, Bukowski E D and Ginzberg D M 1988 *Phys. Rev.* B **38** 11 934
Slakey F, Cooper S L, Klein M V, Price J P and Ginsberg D M 1989 *Phys. Rev.* B **39** 2781
[4] Hackl R, Glaser W, Muller P, Einzel D and Andreas K 1988 *Phys. Rev.* B **38** 7133
[5] Fano U 1961 *Phys. Rev.* **124** 1866

[6] Klein M V, Slakey F, Reznik D, Rice J P and Ginsberg D M 1990 *Phys. Rev.* B **42** 2643
[7] Balkanski M, Sacuto A, Gorochov O, Surryanarayanan R and Correra L 1991 *Proc. High-T_c Superconductor Thin Films, International Conf. on Advanced Materials* ed L Correra (Amsterdam: Elsevier)
[8] Friedl B, Thomsen C and Cardona M 1990 *Phys. Rev. Lett.* **65** 915
[9] McCarty K F, Radousky H B, Liu J Z and Shelton R N 1991 *Phys. Rev.* B **43** 13 751
[10] Schlesinger Z, Collins R T, Holtzberg F, Feild C, Koren G and Gupta A 1990 *Phys. Rev.* B **41** 11 238
[11] Klein M V 1983 *Topics in Applied Physics* vol 8, ed M Cardona (Berlin: Springer) p 149
[12] Balkanski M, Jain K P, Beserman R and Jouanne M 1975 *Phys. Rev.* B **12** 4328
[13] Zawadowski A and Ruvalds J 1970 *Phys. Rev. Lett.* **24** 1111
[14] Kaiser D L, Holtzberg F, Scott B A, McGuire T C 1987 *Appl. Phys. Lett.* **51** 1040
[15] Yu J, Massida S, Freeman A J and Koelling D D 1987 *Phys. Lett.* **122A** 1203
[16] Pickett W E 1989 *Rev. Mod. Phys.* **61** 455
[17] Klein M V and Dierker S B 1984 *Phys. Rev.* B **29** 4976
[18] Dierker S B, Klein M V, Webb G W and Fisk Z 1983 *Phys. Rev. Lett.* **50** 853
[19] Nemetschek R, Staufer T, Misochko O V, Einzel D, Hackl R, Muller P and Andres K 1993 *Electronic Properties of High-T_c Superconductors* ed H Kuzmany, M Mehring and J Fink (Berlin: Springer)
[20] Gurvitch M, Valles J M Jr, Cucolo A M, Dynes R C, Garno J P, Schneemeyer L F and Waszczak J V 1989 *Phys. Rev. Lett.* **63** 1008
[21] Schlesinger Z, Collins R T, Holtzberg F, Feild C, Blandon S H, Welp U, Crabtree G W, Fang Y and Liu J Z 1990 *Phys. Rev. Lett.* **65** 801